Continuous glacier mass changes in High Mountain Asia based on ICESat-1,2 and GRACE/GRACE Follow-on data

Qiuyu Wang[1], Shuang Yi[2], Wenke Sun[1,*]

[1]Key Laboratory of Computational Geodynamics, University of Chinese Academy of Sciences, Beijing 100049, China.

[2]Institute of Geodesy, University of Stuttgart, Stuttgart, Germany

*Corresponding author: E-mail: sunw@ucas.ac.cn

Key points:

1. We provide the first look of ICESat-2 data on glacier thickness and mass changes in the High Mountain Asia.
2. We use independent data from satellite gravimetry to fill data gap of ICESat, and obtain nearly continuous glacier mass changes.
3. There is a quantitative agreement in between satellite gravimetry and satellite altimetry, which show high reliability of result and data

Abstract:

Glacier melt in High Mountain Asia (HMA) is an indicator of climate change, and has a major impact on the regional hydrology and freshwater supply. We determined the recent states of the HMA glaciers based on the first analysis of Ice, Cloud, and Land Elevation Satellite-2 (ICESat-2) data. We used the Gravity Recovery and Climate Experiment (GRACE) and GRACE-FO data to fill the gap of ICESat-1,2 and carry out an independent validation. The agreement between ICESat-1,2 and GRACE/GRACE-FO data at the total and regional scales demonstrates the high reliability of results. Based on ICESat-1,2, the total mass change of the HMA glaciers is -28 ± 6 Gt yr-1 from 2003–2019, which are more negative than stereo imagery based literature. The spatial variability of the glacier indicates rapid thinning in Nyaingentanglha but a slight increase in West Kunlun. ICESat-2 enable new insight into the continuous measurement of the HMA glacier.

Plain abstract:

High Mountain Asia is the largest ice-covered region outside the polar regions. Glaciers have been melting for the past decades due to global warming and the melting will probably continue in the coming decades. This will threaten the water availability in downstream basins and affect the regional or global climate. Thus, it is important to continuously monitor the states of the glaciers. In this study, the first analysis of data released after the launch of the second generation of the Ice, Cloud, and Land Elevation Satellite (ICESat-2) is provided. The data were used to survey the glacier thickness and mass change in High Mountain Asia. We used independent gravity satellite data to fill the gap of ICESat, The two independent datasets agree with respect to the continuous glacier mass change, which indicates the high reliability of the results. Based on our results, the continuous glacier mass change from 2003–2019 is on average -28 ± 6 Gt yr^{-1} (Gt = 10^9 t water) or -0.34 ± 0.07 m yr^{-1} (thickness change). The regional variability of the glaciers ranges from -1.07 ± 0.10 m yr^{-1} in southeastern Nyaingentanglha to +0.16 ± 0.10 m yr^{-1} in West Kunlun.

1. Introduction

High Mountain Asia (HMA) contains the largest ice-covered region outside the south and north poles (*Qiu*, 2008). Meltwater from glaciers and snow, the head of several large rivers, is a major source of drinking water and irrigation for several hundred million people (*Immerzeel and Bierkens*, 2012). Recent reports revealed that these glaciers have been dwindling for the past several decades (*Bolch et al.*, 2012; *Yao et al.*, 2012; *Azam et al.*, 2018; *Yao et al.*, 2019). Future projections indicate that glacier shrinkage due to global warming will continue in the coming decades, which will aggravate the regional water scarcity, especially in subhumid to arid climates, thus affecting economic activities and the political stability (*Pritchard*, 2019). Strategies for the continuous monitoring the states of glaciers are therefore critical for climate change studies and the local management of water resources (*Immerzeel et al.*, 2020). Compared with the interpolation of *in situ* measurements and physical glacier change models, satellite observations are more effective in surveying large-scale glaciers in remote areas crossing political boundaries. The results of numerous studies indicated the practical application of satellite data. Satellite strategies can be divided into two categories:

1) Measurement of geometry including surface height and area. Satellites detecting height changes include laser altimetry (i.e., Ice, Cloud, and Land Elevation Satellite ICESat (*Neckel et al.*, 2014; *Wang et al.*, 2017a; *Treichler et al.*, 2019) and satellite stereo imagery (i.e., SPOT and ASTER; (*Gardelle et al.*, 2012; *Gardelle et al.*, 2013).

2) Measurement of the Earth's gravity field. Satellite gravimetry data from the Gravity Recovery and Climate Experiment (GRACE) were used to calculate the mass change (*Velicogna*, 2009; *Matsuo and Heki*, 2010; *Jacob et al.*, 2012; *Yi et al.*, 2016).

For the first time since the terrain correction method has been proposed for ICESat data processing ICESat data analysis, the thickness changes in the Himalaya and surrounding regions were analyzed (*Kääb et al.*, 2012). Subsequent ICESat-based research considered additional areas and clustering algorithms. The glacier mass loss from 2003–2008/2009 was estimated to be -20 to -24 Gt/yr in the Tibetan Plateau and -24 to -29 Gt yr^{-1} in the HMA (Tibetan Plateau and Tien Shan; (*Gardner et al.*, 2013; *Treichler et al.*, 2015; *Wang et al.*, 2018). The short operational period of ICESat-1 and sparse spatial sampling led to potential large bias. Since the launch of ICESat-2 in 2018, the temporal coverage has been significantly expanded.

In satellite stereo imagery-based studies, the difference between Digital Elevation Models (DEM) is calculated or linear regression is applied to time series of DEM pixels derived from stereo imagery (*Brun et al.*, 2017; *Shean et al.*, 2020). Compared with ICESat, stereo imagery-based studies have a higher spatial coverage and longer time span. Earlier stereo imagery-based studies only covered glaciers in parts of the HMA (*Gardelle et al.*, 2012; *Gardelle et al.*, 2013). Burn et al. (2017) recently calculated a mass change of 92% at a rate of -16 ± 4 Gt yr^{-1} for the glacier area in the HMA from 2000 to 2016. Shen et al. (2020) used stereo imagery data and

estimated that the HMA glacier mass has changed by approximately -19 ± 3 Gt yr^{-1} from 2000–2018. Note that these mass budgets are less negative than those of most previous studies. Limited by the number of available DEMs, satellite stereo imagery has a low temporal resolution. Few time series of glacier mass/thickness changes are based on satellite stereo imagery, which makes it difficult to continuously monitor recent glacier states and the strong temporal variability.

Satellite gravimetry data from GRACE provides monthly Earth gravity fields, demonstrating the feasibility of the use of GRACE data for the monitoring of glaciers, ice caps, water storage in global basins, and sea level changes. The difficulty of the application of GRACE in HMA is mainly due to the strong influence of terrestrial water storage such as increasing water storage of lakes in the Inner Tibetan Plateau (ITP). Early GRACE-based studies reported a glacier mass loss ranging from -47 to -4 Gt/yr from 2003 to 2009/2010 due to the misinterpretation of other hydrological mass changes (*Matsuo and Heki*, 2010; *Jacob et al.*, 2012). Based on more contributions and cautious verifications by scholars, the updated mass budget of HMA glaciers varied from -29 to -19 Gt yr^{-1} in the period 2003–2009 (*Gardner et al.*, 2013), from -35 to -17 Gt yr^{-1} during 2003–2013 (*Schrama et al.*, 2014; *Yi and Sun*, 2014), and from -24 to -18 Gt yr^{-1} in the period of 2003–2015/2016 (*Wang et al.*, 2018; *Wouters et al.*, 2019).

These studies were mostly carried out in variable, short time periods, which makes it difficult to compare the estimates and establish a consensus. Compared with glacier mass budgets, the time series of glaciers include detailed information on the glacier evolution and can be used to quantify the acceleration or deterioration of recent glacier changes. Similarly, the time series of glaciers provide more constraints for the calibration of the prediction models that are used for the projection of the relationship between glaciers and climate change. In a more recent study using GRACE and GRACE Follow-on (FO) data, the HMA glacier loss was estimated at a rate of -29 ± 12 Gt/yr over a longer period from 2002 to 2019 (*Ciracì et al.*, 2020). To confirm the reliability of GRACE/GRACE-FO and fill the data gap, the authors determined the glacier surface mass balance using independent data from the NASA Modern-Era Retrospective Analysis for Research and Application (MERRA-2) reanalysis. The MERRA-2 is the latest atmospheric reanalysis result and is in excellent agreement with GRACE/GRACE-FO at the regional scale of global glaciers and ice caps, except for the HMA glacier. The corrected terms such as GIA, LIA in Ciracì et al. (2020) account for ~60% of the total mass budget of the HMA glaciers. However, the accuracy of these corrections is difficult to assess. It may be cautious when using the corrected terms. Therefore, further studies are required to estimate the mass loss of the HMA glaciers.

In this study, ICESat-1 and 2 data were used for the first time to construct the glacier surface elevation in the HMA for the periods 2003–2009 and 2018–2019. The data were combined with GRACE and GRACE-FO to fill data gaps. Our aim was to establish a consensus based on long time series of glacier mass/thickness changes

(2003–2019) in the whole HMA area and its four subdivisions. We determined the change in the HMA glacier thickness during the period 2003–2019 based on two generations of altimetry satellites, that is, ICESat-1,2. More recent glaciers were analyzed using two dependent satellites.

2. Data and method

2.1 ICESat-1 and ICESat-2 data

The ICESat-2 is the second generation of the laser altimeter ICESat mission, which was launched in 2018 to measure the ice sheet mass change, cloud and aerosol heights, land topography, and vegetation characteristics (*Markus et al.,* 2017). Similar to the first ICESat mission (ICESat-1), ICESat-2 also is also equipped with a laser altimeter, that is, the Advanced Topographic Laser Altimetry System (ATLAS), which utilizes laser pulses that bounce off the Earth's surface, return to the satellite, and record the traffic time pulses. To more accurately measure the Earth's surface height, the ICESat-2 laser is split into six beams. Compared with the laser on ICESat-1, which sends 40 pulses per second, ICESat-2's laser is fast-firing and sends 10,000 pulses per second (Neumann et al., 2018, 2019). Thus, ICESat-2 has a denser footprint than ICESat-1.

Our analysis of the changes in the thickness of the HMA glacier is based on the ICESat-2 L3A Land Ice Height (ATL06). This dataset includes geolocated land-ice surface heights (above the WGS 84 ellipsoid) and ancillary parameters, which are used to interpret and assess the quality of the surface heights (*Smith et al.*, 2020). Over the ice sheet interior, the accuracy of ATL06 is better than 3 cm and the precision of surface measurements is better than 9 cm (*Brunt et al.*, 2019). Similarly, ICESat-1 data were used for the period 2003–2009 in this study. We used the Global Land Surface Altimetry Data (GLA14) of ICESat-1.

The preprocessing was described in Wang et al. (2017b) and is similar to that reported in other studies (*Gardner et al.*, 2013; *Farinotti et al.*, 2015): extraction of the footprint, height conversion, determination of the elevation difference (ICESat and Shuttle Radar Topography Mission, SRTM), and removal of outliers. The calculation of the average change in the glacier thickness is based on the elevation bin method (*Wang et al.*, 2017b). The idea of this method is that 1) the elevation differences between ICESat footprints and SRTM are defined as *dh* (one valid ICESat footprint corresponding to one *dh* value); 2) glaciers are divided into numerous elevation bins according to their altitude distribution; 3) the elevation difference of each bin (defined as *Dh*) equals the median of all footprints' *dh* values in this bin (one elevation bin corresponding *to one Dh*); and 4) the elevation difference of the entire glacier (defined as *DH*) is the area-weighted *Dh* of all bins. We repeated the calculation for different bin widths ranging from 100 to 600 m spaced at 100 m intervals. The final result is the average bin width. The *DH* change is a time series of the glacier thickness. Glacier thickness changes are converted to mass changes using a

density of 850 kg m^{-3} (*Huss*, 2013) which is appropriate for a wide range of conditions.

2.2 GRACE and GRACE-FO data

In this study, the latest releases of the monthly GRACE and GRACE-FO Release-6 (RL06) Stokes coefficients from 2003 to 2020 from the Center for Space Research at the University of Texas (CSR) were used (*Bettadpur*, 2012). The low-degree term of GRACE was processed for consistency with all other GRACE solutions used in the science community. The degree 1 terms are based on a combination of GRACE and ocean model outputs (*Swenson et al.*, 2008). The degree 2 order 0 spherical harmonic coefficient uses satellite laser ranging to replace the GRACE coefficient (*Cheng et al.*, 2013).

The glacier mass change time series were calculated using the least-squares mascon approach of Yi and Sun. (2014). Each mascon is an arbitrarily defined area consisting of 0.5° × 0.5° latitude cells. The distribution of the mascons was optimized to follow the distribution of the glacier. We also placed mascons in the surrounding region to alleviate or separate the leakage of other mass sources. The total water storage estimated by GRACE is composed of the soil moisture storage, groundwater storage, glacial isostatic adjustment (GIA), and unknown sources. In this study, land water and GIA models were used to estimate the soil moisture storage and GIA components, respectively.

2.3 Ancillary data

1) DEM data

Because of large cross-track gaps and rough terrain in the HMA region, a full-area DEM reference can be used to correct topographic differences in ICESat sampling footprints (*Kääb et al.*, 2012). In this study, the DEM from the SRTM (*Farr et al.*, 2007) 1 Arc-Second Global elevation data provided was used, similar to previous research.

2) Glacier boundary data

To distinguish glaciers from land, the latest version of the Randolph Glacier Inventory 6.0 (RGI6.0) was used in this study (*Pfeffer et al.*, 2014), which is based on a Global Land Ice Measurements from Space (GLIMS) project (RGI Consortium 2017).

3) Soil water model

Because of the leakage of other hydrological signals, the soil water model was provided by the Global Land Data Assimilation System (GLDAS) to separate the soil water components from the total mass. The soil water storage model extends to a depth of several meters at a high resolution and in near real time. The GLDAS-2.1 model was used in this study (*Rodell and Beaudoing*, 2016).

4) GIA model

A GIA model was applied based on the model ICE6G to separate the GIA effect (*Argus et al.*, 2014; *Peltier et al.*, 2015). This model was used to calculate geodetic and geologic signals of the Earth such as the rate of radial displacement.

3. Results

The gravity signal of GRACE in the ITP is dominated by increasing masses of lakes, groundwater, and soil water (*Zhang et al.*, 2013; *Wang et al.*, 2016), which is contrary to the glacier change based on field observations (*Yao et al.*, 2012). Therefore, in this study, glaciers in the ITP are excluded from the GRACE-based estimate of the HMA glacier mass change. Most HMA glaciers are distributed on the periphery of the Tibetan Plateau, accounting for 85% of the total HMA glacier area. These peripheral glaciers can be divided into four subregions. Mascons were placed in these areas (Fig. 1a).

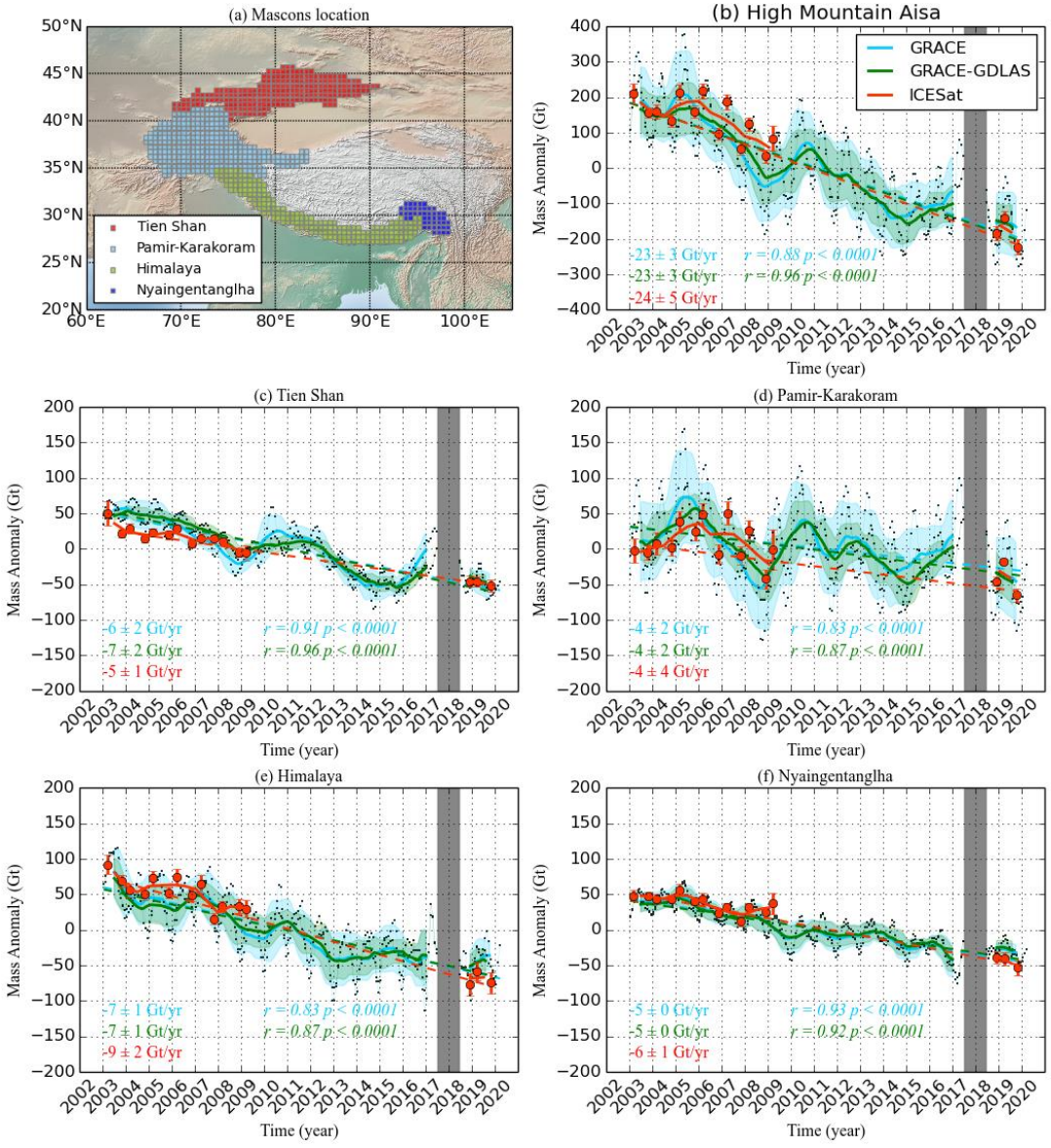

Figure 1. Mascon partitions for the HMA glacier (a) and time series of glacier mass changes in four subregions (c, d, e, f) and their sum (b). A one-year average sliding window is applied to GRACE (solid blue line), GRACE-GLDAS (solid green line), and ICESat-derived glacier mass (solid red line). The colored value is the changing rate based on the linear regression model. The color corresponds to the line color. The *r* value is Pearson's correlation coefficient between ICESat and GRACE(blue *r*)/GRACE-GLDAS(green *r*). The parameter 1-*p* presents the provability of the pass correlation test.

3.1 Continuous time series of the glacier mass change

We constructed time series of the glacier mass change based on GRACE and ICESat for the four subregions (Figs 1c–f). Their sum is shown in Fig. 1b. A one-year average sliding window was applied to improve the signal-to-noise ratio, similar to most GRACE-based studies. We removed the soil moisture based on the GLDAS model (Fig. 1, green line) to isolate the glacier signals. The correlation coefficients were calculated to quantify the consistency between ICESat and GRACE-derived glacier mass changes. Based on the comparison of the results, three key points can be discussed.

1. The data gap between ICESat-1 and 2 was filled with GRACE data, although GRACE data also have a one-year data gap. The ICESat-based glacier mass changes agree with those of GRACE with respect to the changing trends and interannual fluctuations. The agreement is better in the whole HMA area (except for ITP) than in the subregions.
2. After removing the soil moisture from GRACE-based mass changes (i.e., GRACE-GDLAS), the agreement with the ICESat result significantly increased. The GRACE-based mass change includes ample surface snow or land water caused by short-term precipitation. The GDLAS model contains the part mass; thus, the GRACE-GDLAS result is more consistent with the ICESat observation than the GRACE result alone.
3. The GLDAS-based soil moisture does not show a significant trend; thus, the mass change trends of GRACE-GLDAS and GRACE are similar. This might be reasonable. The soil moisture might only fluctuate seasonally and show no trend over a long period.

3.2 Total glacier mass budget

We only used ICESat data and calculated the ITP glacier change to be approximately -4 ± 2 Gt yr^{-1} (Fig. S1). The total mass change of the HMA glacier is -28 ± 6 Gt yr^{-1} (-0.29 ± 0.06 m w.e. yr^{-1}, -0.34 ± 0.07 m yr^{-1}) based on ICESat-1,2 from March 2003 to November 2019. The glacier mass loss in the HMA from 2003–2019/2020 excluding the ITP region is -24 ± 6 Gt yr^{-1} based on ICESat and -23 ± 3 Gt yr^{-1} based on GRACE. After removing the GIA effect, the GRACE-based mass budget of the glacier becomes -28 ± 3 Gt yr^{-1}.

3.3 Spatial variability of the change in the glacier thickness

We present the detailed spatial distribution of the change in the glacier thickness in a 1°× 1° grid based on ICESat-1,2 (Fig. 2). From 2003–2019, the change trend of regional glaciers varied from -1.07 ± 0.10 m yr^{-1} in Nyaingentanglha to +0.14 ± 0.10 m yr^{-1} in West Kunlun, indicating a large regional variability of the glacier change. The HMA glaciers exhibit a strong heterogeneity. Generally, the glacier thickness increases from the Westerly-dominated zone Pamir–Karakoram (-0.10 ± 0.10 m yr^{-1}) to the two edges, that is, Tien Shan (-0.50 ± 0.10 m yr^{-1}) in the northeast and Himalaya (-0.59 ± 0.10 m yr^{-1}) and Nyaingentanglha in the southeast.

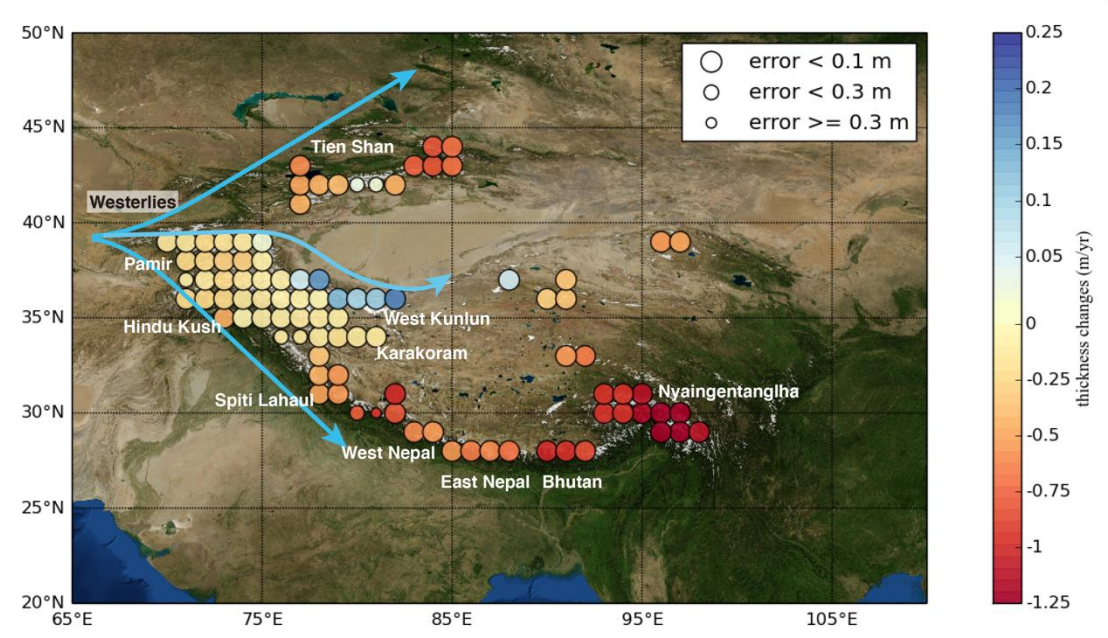

Figure 2. Glacier thickness changes in High Mountain Asia (2003–2019). Map of the average glacier thickness change on a 1° × 1° grid covering rectangular averaging cells of 2° × 2°. The change trend was obtained by the linear regression of data from the autumn campaign of ICESat-1,2. The background is ESRI imagery World from ArcGIS Online.

4. Discussion

4.1 Comparison with other recent studies

Based on efforts regarding the estimation of HMA glaciers, the spatial variability of the glacier changes could be well established. The results of several studies indicated the fastest melting for the Nyaingentanglha glacier, fewer changes in Karakoram, and positive changes in West Kunlun (*Kääb et al.,* 2015; *Brun et al.*, 2017; *Shean et al.*, 2020). However, the change trend in several subregions and whole HMA remains controversial.

1) Comparison with GRACE/GRACE-FO-based studies

Overall, the mass budget determined for the HMA in this study, that is, approximately -28 Gt yr^{-1}, based on ICESat-1,2 is similar to -29 Gt yr^{-1} reported in

recent work based on GRACE/GRACE-FO (*Ciracì et al.*, 2020). Actually, the estimate of Ciracì et al. (2020) includes other hydrological signals, such as lake water in the ITP. They report +2 Gt yr^{-1} compared with -4 Gt yr^{-1} determined based on ICESat-1,2 in this study. Excluding the ITP glacier, we obtained -23 ± 3 Gt yr^{-1} based on GRACE and -24 ± 6 Gt yr^{-1} based on ICESat-1,2 compared with -32 ± 6 Gt yr^{-1} reported in Ciracì et al. (2020). Note that the corrected terms (GIA, hydrological leakage) in Ciracì et al. (2020) are relatively large (approximately -18 Gt yr^{-1}) and thus greatly affect the final result, accounting for ≥60% of the total mass budget. Only GRACE result is -10/-18 Gt yr^{-1} in the HMA/HMA (excluding the ITP) in Ciracì et al. (2020). Our GRACE or GRACE-GLDAS based mass change is in better agreement with ICESat-based estimates than the value after removing the corrected terms such as GIA. Thus, one must be cautious when using the corrected terms based on the tectonic model.

1) Comparison with satellite stereo imagery-based studies

Our result (-28 ± 6 Gt yr^{-1}) for the period 2003–2019 is more negative than that reported for the periods 2000–2016 (-16 ± 4 Gt yr^{-1}; *Brun et al.*, 2017) and 2000–2018 (-19 ± 3 Gt yr-1; *Shean et al.*, 2020). To analyze the divergence and directly compare it with satellite stereo imagery, we followed the division of Brun et al. (2017) and Kääb et al. (2015). The glacier thickness change was determined to avoid uncertainty caused by the volume-to-mass conversion. Compared with Brun et al. (2017), the glacier thickness changes in six of the eleven regions are within two standard deviations (±2 sigma), as shown in Fig. 3 and Table S1. The remaining five regions are West Nepal, East Nepal, Bhutan, Nyaingentanglha, and the ITP. The largest divergence was observed in Bhutan with a 2400 km^2 glacier area. The number of available data might be affected by a small subregion. Compared with recent stereo imagery-based work (*Shean et al.*, 2020), the period 2000–2018 is close to that used in our studies. Nine of eleven regions are within two standard deviations. The increase in the percentage is due to improved performances in the ITP (significant improvement), West Nepal, and East Nepal. This difference is partly due to the different study periods. In general, ICESat-1,2-based results are more negative than satellite stereo imagery-based results, especially in areas with rapidly thickening glaciers such as the southeastern Himalaya (Nepal and Bhutan) and Nyaingentanglha.

2) Comparison with ICESat-1-based studies

Six out of the eleven subregions are within two standard deviations. Considering the short period (2003–2008) of previous ICESat-1-based studies, the difference might be due to glacier changes in the recent decade. We present the glacier thickness changes based on ICESat-1 for comparison (Fig. 3 and Table S1). Our results are in good agreement with those of previous studies in nine of eleven regions. The two divergent regions are the Bhutan and East Nepal (called Everest in Kaab et al., 2015) glaciers. Based on our work, these two subregions are relatively small, that is, ~2400 and 4900 km^2. These values contrast those reported by Kaab et al. (2015) are 3500 and 8500 km^2, respectively. The large difference in the division and glacier inventory

might be the reason for the different estimates. If we treat the two subregions as one subregion, the divergence improves by approximately -0.63 m yr^{-1} in this study and -0.52 m yr^{-1} in Kaab et al. (2015). In total, ICESat-1- and ICESat-1,2-based results demonstrate a strong ablation in Nyaingentanglha/Bhutan, that is, thickness changes of ~1 m yr^{-1}, which are more negative than the results obtained from satellite stereo image-based studies.

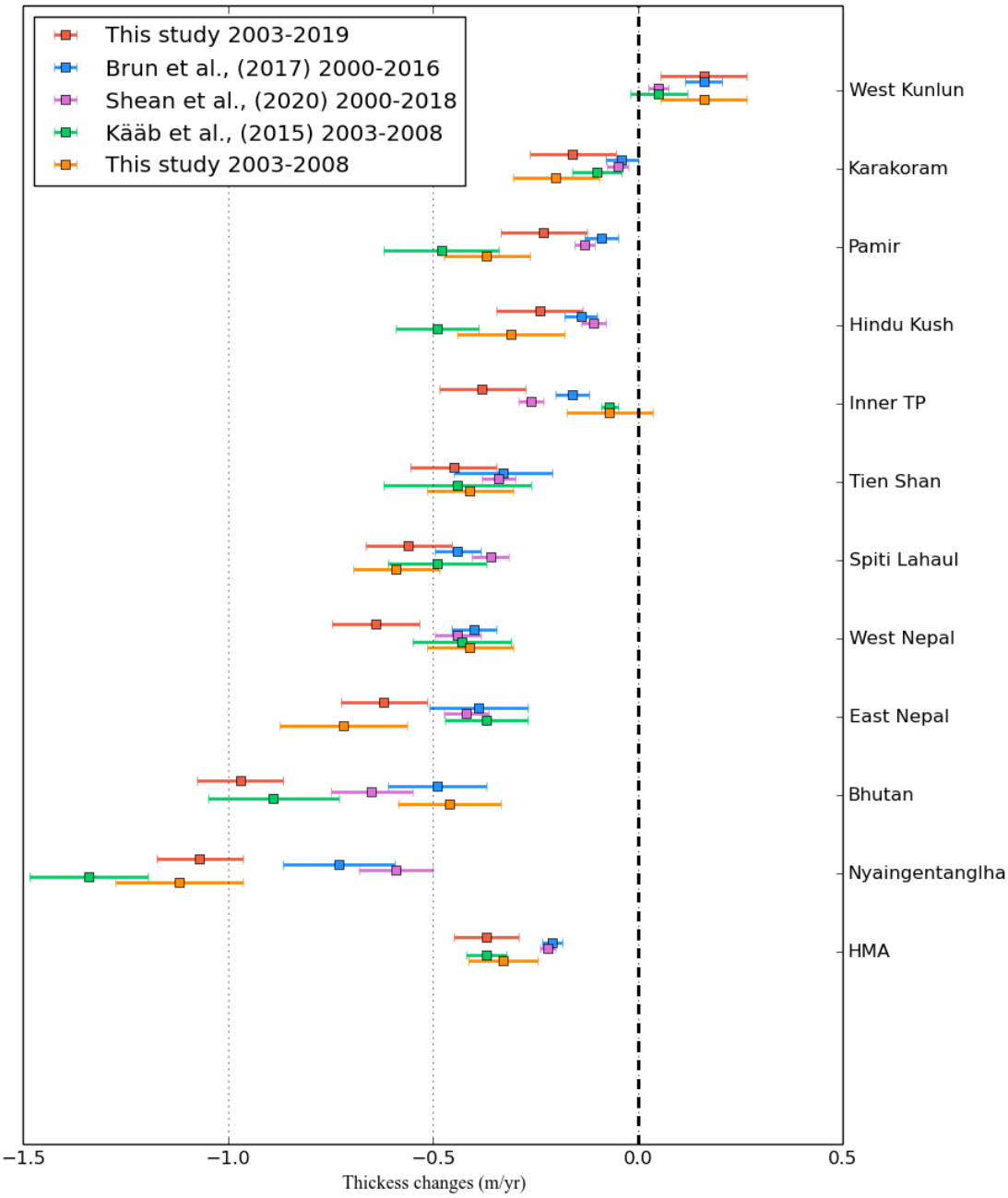

Figure 3. The comparison of glacier thickness changes from this study and previous results. The Errors are given at the 1σ level. Kääb et al., (2015) did not provide the glacier trend in inner TP, Tien Shan, but Brun et al., (2017) provide missing value by use same method of Kääb et al., (2015).

4.2 Error analysis and choice of hyperparameters

The uncertainty calculation of *DH* (error bar in Fig. 1) follows Wang et al. (2017b):

$$\sigma_{DH} = \sqrt{\sigma_{std}^2 + {\sigma_{dh}}^2}, \qquad (1)$$

where σ_{std}^2 is the standard deviation of the parameters for the different widths of elevation bins ranging from 100 to 600 m spaced at 100 m intervals; ${\sigma_{dh}}^2$ is the error of *dh* due to vertical SRTM (7–12 m), ICESat errors, and radar penetration; and ${\sigma_{dh}}^2$ was set to 20 m based on the footprint in this study.

The total uncertainty of the glacier mass budget consists of three parts*: 1) autumn DH* trend, 2) glacier area uncertainty, and 3) uncertainty in the density assumption. We considered an uncertainty of 10% for the glacier area and density. The autumn trend was estimated using Eq. (2):

$$\sigma_{DH/dt} = \sqrt{\sigma_{fit}^2 + \sigma_{spat}^2 + \sigma_{temp}^2 + \sigma_{bais}^2}, \quad (2)$$

where ${\sigma_{dh}}^2$ is the linear fitting error, σ_{apat}^2 and σ_{temp}^2 are the irregular spatial and temporal ICESat sampling errors, respectively; and σ_{bais}^2 is the unknown systematic uncertainty considering intercomparison biases and crustal uplift. In this study, σ_{spat}^2, σ_{temp}^2, and σ_{bais}^2 were set to 0.06, similar to previous studies (*Gardner et al.,* 2013; *Farinotti et al.,* 2015).

1) Spatial glacier coverage

The ICESat measurement of the changes in the glacier thickness only covers the region with footprints. Therefore, extrapolation to the whole glacier area is necessary. In this study, the extrapolation was carried out as follows: 1) The mean altitude (h_g) and standard deviation (h_{std}) of the glaciers in each subregion were calculated. The results of ~95% of the glaciers with altitudes ranging from $h_g - 2h_{std}$ to $h_g + 2h_{std}$ were determined in their corresponding elevation bin (see glacier altitude histogram Fig. S2). The extrapolation was based on the assumption that glaciers in the same elevation range exhibit the same changes; and 2) the remaining ~5% of glaciers were added to the calculation of the mass budget and the results of 95% of the glaciers were used.

2) Linear regression and ICESat observation campaign

Due to strong snowfall or snowpack in winter, the winter campaign of ICESat was not used for the linear regression in most previous ICESat-based studies of HMA glaciers. In this study, all glacier change trends (Figs 1 and 2, Table S1) are based on the linear regression of the ICESat autumn campaign. Note that the result of the ICESat winter campaign is presented in Fig. 1; however, it was not used for the regression model. Due to the long temporal span after the combination of ICESat-1 and 2, the linear regressions without or with the winter campaign insignificantly differ. In addition, to maintain consistency with the ICESat-1 observation, we used the same time window to obtain the autumn and winter observation of ICESat-2. Although the

downsampling of ICESat-2 will lead to the loss of data, it helps to reduce the bias in the mass budget evaluation and keep consistency with ICESat-1.

5. Conclusions

This study demonstrates the first results on recent glacier surface changes in the HMA region based on ICESat-2. The total mass balances and changes in the thickness of the HMA glacier from 2003–2019 (~17 years) were determined by combining ICESat-1 and 2. We used GRACE data to fill the data gap of ICESat-1,2 from 2010 to 2017 and provided a continuous time series of the glacier mass change in the HMA and its four subregions. The comparison of ICESat-1,2 and GRACE/GRACE-FO shows that these data are in excellent agreement at the total and regional scales (r = *0.9*, $p < 0.0001$). This consistency between the two independent approaches indicates the high reliability of HMA glacier mass change data and validates the calculations based on two sets of satellite observations. Based on this study, that is, the use of ICESat-1,2 data from March 2003 to November 2019, the total mass budget of the HMA glaciers is -28 ± 6 Gt yr^{-1}. On the periphery of the Tibetan Plateau, including Tien Shan, Pamir–Karakoram, Himalaya, and Nyaingentanglha, the mass budget of the glaciers in the period 2003 to 2019/2020 is -24 ± 5 Gt yr^{-1} based on ICESat, -23 ± 3 Gt yr^{-1} based on GRACE, and -28 ± 3 Gt based on GRACE with GIA-corrected terms. Based on the spatial heterogeneity of the glacier change rates, the most negative value is observed in Nyaingentanglha (-1.07 ± 0.10 m yr^{-1}), followed by the Himalayas (-0.58 ± 0.10 m yr^{-1}), Tien Shan (-0.45 ± 0.10 m yr^{-1}), and Pamir–Karakoram (−0.10 ± 0.10 m yr^{-1}). The West Kunlun glaciers slightly increased by approximately +0.16 ± 0.10 m yr^{-1}. Based on ICESat2 and GRACE-FO, the HMA glacier changes can be continuously monitored.

6. Acknowledgements

We are grateful for the financial support from the Natural Science Foundation of China (41774088, 41974093, 41331066, and 41474059), Key Research Program of Frontier Sciences of the Chinese Academy of Sciences (QYZDY-SSW-SYS003), and fellowships of the China Postdoctoral Science Foundation (2020M670424 and 2020T130641). The data used in this study are publicly open, and their sources are indicated in the “Data and Method” section. ICESat-1,2 data are provided by National Snow & Ice Data Center and available at the website (https://nsidc.org/data/icesat and https://nsidc.org/data/icesat-2). GRACE and GRACE-FO data are provided by the University of Texas and available at the website (http://www2.csr.utexas.edu/grace/). The GLDAS-2.1 data are available at the website (https://disc.gsfc.nasa.gov/datasets/GLDAS_NOAH025_3H_2.1/summary).

REFERENCES

Argus, D. F., W. R. Peltier, R. Drummond, and A. W. Moore (2014), The Antarctica component of postglacial rebound model ICE-6G_C (VM5a) based on GPS positioning, exposure age dating of ice thicknesses, and relative sea level histories, *Geophysical Journal International*, *198*(1), 537-563, doi:10.1093/gji/ggu140.

Azam, M. F., P. Wagnon, E. Berthier, C. Vincent, K. Fujita, and J. S. Kargel (2018), Review of the status and mass changes of Himalayan-Karakoram glaciers, *Journal of Glaciology*, *64*(243), 61-74, doi:10.1017/jog.2017.86.

Beaudoing H, Rodell M. GLDAS Noah Land Surface Model L4 3 hourly 0.25× 0.25 degree V2. 1[J]. Goddard Earth Sciences Data and Information Services Center (GES DISC): Greenbelt, MD, USA, 2016.

Bettadpur, S. (2012). UTCSR level‐2 processing standards document, technical report GRACE. Austin, Texas: Center for Space Research, University of Texas.

Bolch, T., A. V. Kulkarni, A. Kaab, C. Huggel, F. Paul, J. G. Cogley, H. Frey, J. S. Kargel, K. Fujita, and M. Scheel (2012), The State and Fate of Himalayan Glaciers, *Science*, *336*(6079), 310-314.

Brun, F., E. Berthier, P. Wagnon, A. Kääb, and D. Treichler (2017), A spatially resolved estimate of High Mountain Asia glacier mass balances from 2000 to 2016, *Nature Geoscience*, *10*(9), 668-673, doi:10.1038/ngeo2999.

Brunt, K. M., T. A. Neumann, and B. E. Smith (2019), Assessment of ICESat-2 Ice Sheet Surface Heights, Based on Comparisons Over the Interior of the Antarctic Ice Sheet, *Geophysical Research Letters*, *46*(22), 13072-13078, doi:10.1029/2019gl084886.

Cheng, M., J. Ries, and B. Tapley (2013), Geocenter variations from analysis of SLR data, in *Reference Frames for Applications in Geosciences*, edited, pp. 19-25, Springer.

Ciracì, E., I. Velicogna, and S. Swenson (2020), Continuity of the Mass Loss of the World's Glaciers and Ice Caps From the GRACE and GRACE Follow-On Missions, *Geophysical Research Letters*, *47*(9), e2019GL086926, doi:10.1029/2019gl086926.

Farinotti, D., L. Longuevergne, G. Moholdt, D. Duethmann, T. Mölg, T. Bolch, S. Vorogushyn, and A. Güntner (2015), Substantial glacier mass loss in the Tien Shan over the past 50 years, *Nature Geoscience*.

Farr, T. G., et al. (2007), The Shuttle Radar Topography Mission, *Reviews of Geophysics*, *45*(2), RG2004, doi:10.1029/2005rg000183.

Gardelle, J., E. Berthier, and Y. Arnaud (2012), Slight mass gain of Karakoram glaciers in the early twenty-first century, *Nature Geoscience*, *5*(5), 322-325, doi:10.1038/ngeo1450.

Gardelle, J., E. Berthier, Y. Arnaud, and A. Kaab (2013), Region-wide glacier mass balances over the Pamir-Karakoram-Himalaya during 1999-2011 (vol 7, pg 1263, 2013), *The Cryosphere*, *7*(6), 1885-1886, doi:10.5194/tc-7-1885-2013.

Gardner, A. S., et al. (2013), A Reconciled Estimate of Glacier Contributions to Sea Level Rise: 2003 to 2009, *Science*, *340*(6134), 852-857, doi:10.1126/science.1234532.

Huss, M. (2013), Density assumptions for converting geodetic glacier volume change to mass change, *The Cryosphere*, *7*(3), 877-887.

Immerzeel, W. W., and M. F. P. Bierkens (2012), Asia's water balance, *Nature Geosci*, *5*(12), 841-842.

Immerzeel, W. W., et al. (2020), Importance and vulnerability of the world's water towers, *Nature*, *577*(7790), 364-369, doi:10.1038/s41586-019-1822-y.

Jacob, T., J. Wahr, W. T. Pfeffer, and S. Swenson (2012), Recent contributions of glaciers and ice caps to sea level rise, *Nature*, *482*(7386), 514-518, doi:http://www.nature.com/nature/journal/v482/n7386/abs/nature10847.html#supplementary-information.

Kääb, A., E. Berthier, C. Nuth, J. Gardelle, and Y. Arnaud (2012), Contrasting patterns of early twenty-first-century glacier mass change in the Himalayas, *Nature*, *488*(7412), 495-498, doi:10.1038/nature11324.

Kwok, R., G. Cunningham, T. Markus, D. Hancock, J. H. Morison, S. P. Palm, S. L. Farrell, A. Ivanoff, J. Wimert, and the ICESat-2 Science Team. 2020. ATLAS/ICESat-2 L3A Sea Ice Height, Version 3. [Indicate subset used]. Boulder, Colorado USA. NASA National Snow and Ice Data Center Distributed Active Archive Center. doi: https://doi.org/10.5067/ATLAS/ATL07.003. [Date Accessed].

Markus, T., Neumann, T., Martino, A., Abdalati, W., Brunt, K., Csatho, B., Farrell, S., Fricker, H., Gardner, A., Harding, D., Jasinski, M., Kwok, R., Magruder, L., Lubin, B., Luthcke, S., Morison, J., Nelson, R., Neuenschwander, A., Palm, S., Popescu, S., Shum, C., Schutz, B., Smith, B., Yang, Y., & Zwally, J. (2017). The Ice, Cloud, and land Elevation Satellite‐2 (ICESat‐2): Science requirements, concept, and implementation. Remote Sensing of Environment, 190, 260–273. https://doi.org/10.1016/j.rse.2016.12.029

Matsuo, K., and K. Heki (2010), Time-variable ice loss in Asian high mountains from satellite gravimetry, *Earth and Planetary Science Letters*, *290*(1–2), 30-36, doi:http://dx.doi.org/10.1016/j.epsl.2009.11.053.

Neckel, N., J. Kropáček, T. Bolch, and V. Hochschild (2014), Glacier mass changes on the Tibetan Plateau 2003–2009 derived from ICESat laser altimetry measurements, *Environmental research letters*, *9*(1), 014009.

Neumann, T. A., Brenner, A. C., Hancock, D. W., Harbeck, K., Luthcke, S., Robbins, J., Saba, J., & Gibbons, A. (2018). Ice, Cloud, and Land Elevation Satellite-2 project algorithm theoretical basis document for global geolocated photons (ATL03). https://icesat-2.gsfc.nasa.gov/science/data-products.

Neumann, T. A., Martino, A. J., Markus, T., Bae, S., Bock, M. R., Brenner, A. C., Brunt, K. M., Cavanaugh, J., Fernandes, S. T., Hancock, D. W., Harbeck, K., Lee, J., Kurtz, N. T., Luers, P. J., Luthcke, S. B., Magruder, L., Pennington, T. A., Ramos‐Izquierdo, L., Rebold, T., Skoog, J., & Thomas, T. C. (2019). The Ice, Cloud, and Land Elevation Satellite‐2 Mission: A global geolocated photon product. Remote Sensing of Environment, 233, 111325. https://doi.org/10.1016/j.rse.2019.111325

Peltier, W. R., D. F. Argus, and R. Drummond (2015), Space geodesy constrains ice age terminal deglaciation: The global ICE-6G_C (VM5a) model, *Journal of Geophysical Research: Solid Earth*, *120*(1), 450-487, doi:10.1002/2014jb011176.

Pfeffer, W. T., A. Arendt, A. Bliss, T. Bolch, J. G. Cogley, A. S. Gardner, J. O. Hagen, R. Hock, G. Kaser, and C. Kienholz (2014), The Randolph Glacier Inventory : a globally complete inventory of glaciers, *Journal of Glaciology*, *60*(221), 537-552.

Pritchard, H. D. (2019), Asia's shrinking glaciers protect large populations from drought stress, *Nature*, *569*(7758), 649-654, doi:10.1038/s41586-019-1240-1.

RGI Consortium (2017). Randolph Glacier Inventory – A Dataset of Global Glacier Outlines: Version 6.0: Technical Report, Global Land Ice Measurements from Space, Colorado, USA. Digital Media. DOI: https://doi.org/10.7265/N5-RGI-60

Schrama, E. J. O., B. Wouters, and R. Rietbroek (2014), A mascon approach to assess ice sheet and glacier mass balances and their uncertainties from GRACE data, *Journal of Geophysical Research: Solid Earth*, *119*(7), 6048-6066, doi:10.1002/2013jb010923.

Shean, D. E., S. Bhushan, P. Montesano, D. R. Rounce, A. Arendt, and B. Osmanoglu (2020), A Systematic, Regional Assessment of High Mountain Asia Glacier Mass Balance, *Frontiers in Earth Science*, *7*(363), doi:10.3389/feart.2019.00363.

Swenson, S., D. Chambers, and J. Wahr (2008), Estimating geocenter variations from a combination of GRACE and ocean model output, *Journal of Geophysical Research: Solid Earth*, *113*(B8), doi:10.1029/2007jb005338.

Treichler, D., A. Kääb, N. Salzmann, and C. Y. Xu (2019), Recent glacier and lake changes in High Mountain Asia and their relation to precipitation changes, *The Cryosphere*, *13*(11), 2977-3005, doi:10.5194/tc-13-2977-2019.

Treichler, D., C. Nuth, and E. Berthier (2015), Brief Communication: Contending estimates of 2003--2008 glacier mass balance over the Pamir-Karakoram-Himalaya, *The Cryosphere*, *9*, 557.

Velicogna, I. (2009), Increasing rates of ice mass loss from the Greenland and Antarctic ice sheets revealed by GRACE, *Geophysical Research Letters*, *36*(19).

Wang, Q., S. Yi, L. Chang, and W. Sun (2017a), Large-Scale Seasonal Changes in Glacier Thickness Across High Mountain Asia, *Geophysical Research Letters*, *44*(20), 10,427-410,435, doi:10.1002/2017gl075300.

Wang, Q., S. Yi, and W. Sun (2016), The changing pattern of lake and its contribution to increased mass in the Tibetan Plateau derived from GRACE and ICESat data, *Geophysical Journal International*, *207*(1), 528-541, doi:10.1093/gji/ggw293.

Wang, Q., S. Yi, and W. Sun (2017b), Precipitation-driven glacier changes in the Pamir and Hindu Kush mountains, *Geophysical Research Letters*, *44*(6), 2817-2824, doi:10.1002/2017gl072646.

Wang, Q., S. Yi, and W. Sun (2018), Consistent interannual changes in glacier mass balance and their relationship with climate variation on the periphery of the Tibetan Plateau, *Geophysical Journal International*, *214*(1), 573-582, doi:10.1093/gji/ggy164.

Wouters, B., A. S. Gardner, and G. Moholdt (2019), Global glacier mass loss during the GRACE satellite mission (2002-2016), *Frontiers in Earth Science*, *7*, doi:Urn:Nbn:Nl:Ui:10-1874-385100.

Yao, T., et al. (2012), Different glacier status with atmospheric circulations in Tibetan Plateau and surroundings, *Nature Clim. Change*, *2*(9), 663-667, doi:http://www.nature.com/nclimate/journal/v2/n9/abs/nclimate1580.html#supplementary-information.

Yao, T., et al. (2019), Recent Third Pole's Rapid Warming Accompanies Cryospheric Melt and Water Cycle Intensification and Interactions between Monsoon and Environment: Multidisciplinary Approach with Observations, Modeling, and Analysis, *Bulletin of the American Meteorological Society*, *100*(3), 423-444, doi:10.1175/bams-d-17-0057.1.

Yi, S., and W. Sun (2014), Evaluation of glacier changes in high-mountain Asia based on 10 year GRACE RL05 models, *Journal of Geophysical Research: Solid Earth*, *119*(3), 2013JB010860, doi:10.1002/2013jb010860.

Yi, S., Q. Wang, L. Chang, and W. Sun (2016), Changes in Mountain Glaciers, Lake Levels, and Snow Coverage in the Tianshan Monitored by GRACE, ICESat, Altimetry, and MODIS, *Remote Sensing*, *8*(10), 798.

Zhang, G., T. Yao, H. Xie, S. Kang, and Y. Lei (2013), Increased mass over the Tibetan Plateau: from lakes or glaciers?, *Geophysical Research Letters*, *40*(10), 2125-2130.